47TH TURBOMACHINERY & 34TH PUMP SYMPOSIA
HOUSTON, TEXAS | SEPTEMBER 17-20, 2018
GEORGE R. BROWN CONVENTION CENTER

COOLING WATER PUMP STATION OPTIMIZATION USING CFD AND PHYSICAL MODEL TEST

Francesco Annese
Pump Hydraulic Engineering Manager
Baker Hughes a GE Company
Bari, Italy

Letizia Ficele
Pump Lead Testing Engineer
Baker Hughes a GE Company
Bari, Italy

Emanuele Lisanti
Pump Lead Design Engineer
Baker Hughes a GE Company
Bari, Italy

Francesco Annese is team manager of a group dedicated to Centrifugal Pump hydraulic design and technical support to commercial operation for Baker Hughes a GE company. He joined GE in 2007 after 2 years' experience as design engineer for gas metering systems. Mr. Annese holds a M.S degree (mechanical engineering) from the Politecnico di Bari.

Letizia Ficele is a lead testing engineer within Model Test Group supporting Centrifugal Pump hydraulic design team in new hydraulics' design validation within research and requisition jobs for Baker Hughes a GE company. She joined GE in 2015, after several years' experience as testing engineer for automotive applications. Mrs. Ficele holds a M.S degree (mechanical engineering) from the Politecnico di Bari.

Emanuele Lisanti is lead hydraulic design engineer in the Engineering team for Baker Hughes a GE company. He joined GE in 2011 after a 3 years' experience as piping design engineer. Mr. Lisanti holds a M.S degree (mechanical engineering) from the Politecnico di Bari.

ABSTRACT

In this paper, a combined study between Computational Fluid Dynamics (CFD) and a model test has been carried on a Cooling Water Pumping Station as part of a new power plant. Cooling Water Pumping Station is composed of two cooling tower's basins with two penstocks (one per each basin) through which water goes down to the pit, where seven main and two emergency water pumps are installed. The aim of this work was to validate a water pit layout, more compact than required by ASME ANSI HI 9.8 2012 design guidelines [1]. Issues are usually associated with certain undesirable flow characteristics and are caused by poor design of pump intake structure. The CFD simulation has been a useful mean for quick visualization of the physical phenomena that arise in the pit and has given important indications about potential critical areas to focus on. According to ANSI HI 9.8 guidelines, a physical model test of the pumping station has been designed and built-up to define and assess the pump intake flow distribution. The physical model study confirmed the potentially critical turbulence near pump inlet indicated by CFD. Also, the modification investigated and verified thru the CFD study were implemented with the physical model leading to fully improved flow distribution, both inside the sump and at pump bell inlet. Finally, the pit lay out was acceptable for the expected sequences of pumps in parallel operation.

INTRODUCTION

Cooling water pumps are used for supplying heat exchangers with cooling water in various plants, for hydrocarbon processing, oil refinery, chemical processing and power generation. Normally these pumps receive cold water from an external source (sea, lake, river), thru an intake system and route it through the process coolers and condensers having the function to absorb heat from process steam, which need to be cooled or condensed. The pumps operating for cooling water services can be vertical or horizontal, with single stage (single or double suction) or multistage. The head is determined by the type of cooling system and capacity depends from plant output power and number of pumps operating in parallel. In certain case the pump capacity can be very large up to 15000-20000 m3/h (66000-88000 GPM).
For this power plant, the customer request was to check and validate the basin and the penstocks dimensions and lay out, trying to minimize the modifications to existing geometries to have nearly uniform flow field without any recirculation and air bubbles at pump inlet.
It is well known that some type of vortices, which are generated in the intake system and move towards to the pump suction bell can interact with the impeller, causing high vibrations and noise up to unacceptable levels, impacting pump performance and especially reliability. Moreover, flow distribution (uneven velocity distribution) and/or high swirl at the impeller eye can have similar deleterious impact on pump operability and even mechanical failures in discharge piping and plant components. There are field cases reported in the literature [2], which present situation of an acoustic and structural resonance in discharge piping, where the source was originated by flow distribution and high swirl at the pump inlet induced by sump geometry.
In order to prevent such situation, the overall configuration of the entire pump intake system (geometry, water level, number and configuration of pumps operating in parallel) must be optimized. This is a complex process, which is customarily and contractually performed by building a physical model at reduced scale. The number of modifications and variants can be very large involving both long time and high cost. Moreover, the process of optimization is even more difficult when there are constrains given by geometry of intake layout.
In the recent years there is some tendency of using CFD (Computation Fluid Dynamic) for making a "virtual model" of intake and sequence of operational pumps. The CFD study permits to guide the selection of the variants to be interactively (sequence of steps) and ultimately confirmed with the physical model test, as requested by contract.
This paper presents such modern approach with combination of CFD study and series of physical model tests for optimization of a cooling water pumping station with reduced time and lowest cost. The scope of physical model test was not to validate the CFD calculation accuracy, rather CFD was used only to reduce time and cost of physical model tests by decreasing the number of variants and modifications that can influence the entire system behavior.

ANSI HI REQUIREMENTS

Under the proposed cooling water system design, water from two Cooling Tower Basins enters the intake structure through a couple of channels. Each intake channel comprises of a single course trash screen and penstock arrangement. The water discharge from each channel, gravitates to a common cooling water pump basin housing the main circulation and emergency water pumps. Under the current arrangement, a total of seven main water circulation pumps and two smaller emergency cooling water pumps are installed in the common suction sump.
In details the system is composed (Fig.1) by:

- Intake channels dredged to depth contour
- Intake cooling water pump basin to depth contour
- Nr. 7 Cooling Water Circulation double suction pumps, with 5 operating and 2 stand-by (A to G);
- Nr. 2 Emergency cooling water double suction pumps, with 1 operating and 1 stand-by (A' and B');
- Nr. 1 Provision future for one Cooling Water Circulation Pump.

The specific speed of the main pump is 2500 (US units) using half pump capacity (Qeye).
A comparative dimensional check between ANSI-HI 9.8-2012 requirements and pit layout (Fig.1) has been done as per Table 1. For most important parameter as defined by HI standards [1], the terms "OK" means that the parameters (relative to the bell inlet diameter) complies with the HI recommendations, which are given as range or minimum values. The term "NOT OK" means that the parameter deviates, marginally or largely, from the recommended criterion (range, minimum).

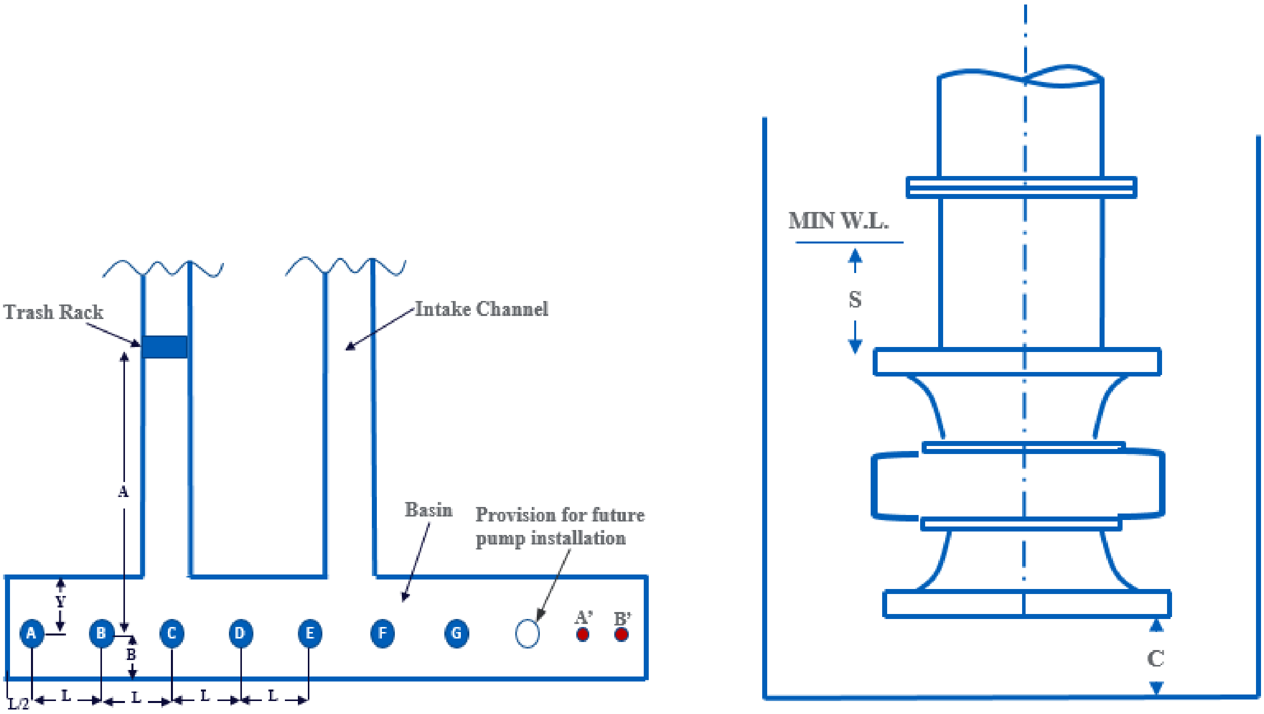

Fig.1 – Overall intake layout.

Table 1 - ANSI HI Dimensional Check.

EMERGENCY PUMP	
Dimensions	**Check**
C'	**OK**
B'	**NOT OK**
L'	**OK**
L'/2	**OK**
S'	**OK**
Y'	**NOT OK**
A'	**OK**

MAINPUMP	
Dimensions	**Check**
C	**OK**
B	**NOT OK**
L	**OK**
L/2	**OK**
S	**OK**
Y	**NOT OK**
A	**NOT OK**

The dimensional check has shown a possible vortex generation inside the basin. Vortices may cause some typical problems such as pump vibrations and noise, decrease of pumps efficiency, unsteady hydraulic loads (axial, radial, torsional), debris and air entraining into the pump basin and ultimately at the impeller eyes. All the above-mentioned adverse effects can lead to a reduction of pumps' reliability and in some cases disruptive interaction with discharge piping. According to ANSI/HI 9.8-2012 flow chart (extract in Fig.2) a model test was required to validate the pit geometry. Therefore, to speed up the physical model test activity, a numerical CFD calculation has been carried out for a preliminary vortex detection and basin optimization.

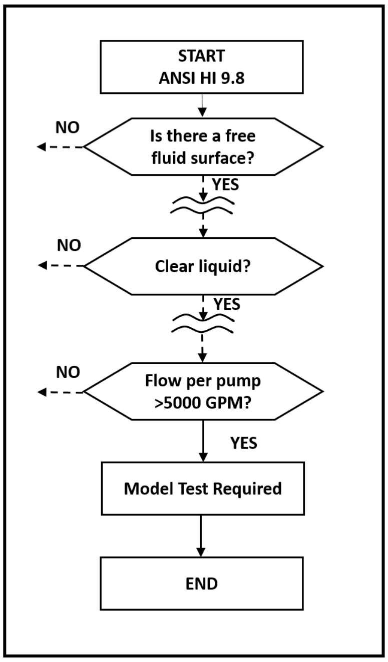

Fig. 2 - ANSI-HI 9.8 -2012 flow chart extract.

CFD CALCULATION AND SCALE MODEL

The numerical study of the cooling water pumping station has been performed to observe the flow path in the adduction channel and pit according to existing geometry.
Due to wide extension of the pumping station at its natural scale and after several evaluations in terms of needed computation time, it has been decided to run CFD model to a scale of 1:5.4 (same scale used for physical model test). In selecting the optimum scale for running CFD model, importance has been given to a range of theoretical considerations regarding the correct representation of flow conditions, which place limits on the minimum size of a model. All following recommendations can be found in ANSI HI 9.8 – 2012.
Models involving a free surface are operated using Froude similarity since the flow process is controlled by gravity and inertial forces. Then, for similarity of flow patterns the Froude number shall be equal in model and prototype.
In addition, in modeling a pump intake to study the potential formation of vortices, it is important to select reasonably large geometric scale to minimize viscous and surface tension scale effects. The scale selection based on vortex similitude considerations is a requirement to avoid scale effects and unreliable results.
It can be shown by the principles of dimensional analysis that flow motions involving vortex formation inside an intake are governed by the following dimensionless parameters [1]:

uD/Γ, $u/(gD)^{0.5}$, D/S, uD/ν, and $u^2D/(\sigma/\rho)$

The influence of viscous effects is defined by the parameter $uD/\nu=Re$, the Reynolds number, and surface tension effects are indicated by $u^2D/(\sigma/\rho)=We$, the Weber number (u = average axial velocity at the bell entrance).

Based on the available literature and ANSI-HI, the influence of viscous forces and surface tension on vortexing may be negligible if the values of Re and We in the model fall above 3x10^4 and 120 respectively ([3], [4]).
With negligible viscous and surface tension effects, dynamic similarity is obtained by equating the parameters uD/Γ, $u/(gD)^{0.5}$ (Froude) and D/S in the model and prototype.
In conclusion, an undistorted geometrically scaled Froude model satisfies this condition, provided that the approach flow

pattern near the sump, which governs the circulation Γ, is properly simulated. A Froude geometrically undistorted 1:5.4 scale model, satisfies all below requirements (Table 2), then representing the optimum compromise in terms of computation time - results accuracy.

Table 2 - Fluid dynamic parameters (*safety factor = 2 applied).

	Froude Number	Reynold's Number	Weber Number	Channel/Sump Width [mm]
Min ANSI Requirement	NA	60000*	240*	300
Model at 1:5.4	3.1	95000	1019	>300

CFD CASE SETUP

A single phase, steady state CFD model has been run for different combinations of pumps in use (Test Matrix in Table 3). All calculations have been performed at the minimum liquid level considered as the worst case.
The geometry and computational mesh were modeled using commercial software (Siemens NX® 8.5 (2012) and Ansys ICEM® (2015)), while all simulations were undertaken with Ansys CFX® v16.2 (2015).

Table 3 - Test matrix.

Test conf.	Pump A	Pump B	Pump C	Pump D	Pump E	Pump F	Pump G	Em.Pump A'	Em.Pump B'
1	O	X	O	X	O	O	O	X	O
2	X	O	X	O	O	O	O	X	O
3	O	O	O	O	X	O	X	O	X
4	O	O	O	X	O	X	O	X	O
5	X	O	O	O	O	O	X	O	X
6	O	X	O	O	O	X	O	X	O
7	O	O	X	O	X	O	O	X	O
8	O	O	O	O	O	X	X	X	O
9	X	X	O	O	O	O	O	O	X
10	X	X	O	O	O	O	O	X	O

O=Running X=Not Running

Main purpose of the study has been the identification of specific hydraulic phenomena that can adversely affect the performance of pumps such as:

- The potential for vortex activity.
- Excessive pre-swirl and highly uneven velocity profile over the limits [1], at location of impeller eye top and bottom, representing potential risks for fluctuating loads on pump impellers, vibration, cavitation, loss of pump capacity and decreasing efficiency.
- Low fluid velocities zones at impeller eyes.

The CFD simulation is a useful mean for quick visualization of the flow field profiles through the pumping station, and helps

reducing testing time as it gives important indications about potential critical areas to focus on and possible problems solutions.
The computational domain for the pumping station is shown in Figure 3. The grid dimension was optimized, in order to obtain an acceptable calculation time without compromising the accuracy of final results. For this reason, the use of a single domain (18 million elements - tetrahedral mesh) including pump casing (without impeller) and discharge pumps column, channels and the pit was helpful to reduce mesh size. All the calculations were run on a cluster domain by using 24 to 36 processors.
Following boundary conditions have been applied:

- Mass flow rate at inlet channel (half of total flow for each channel)
- Static pressure at pumps domain outlet
- No slip wall condition for pit walls and channel walls

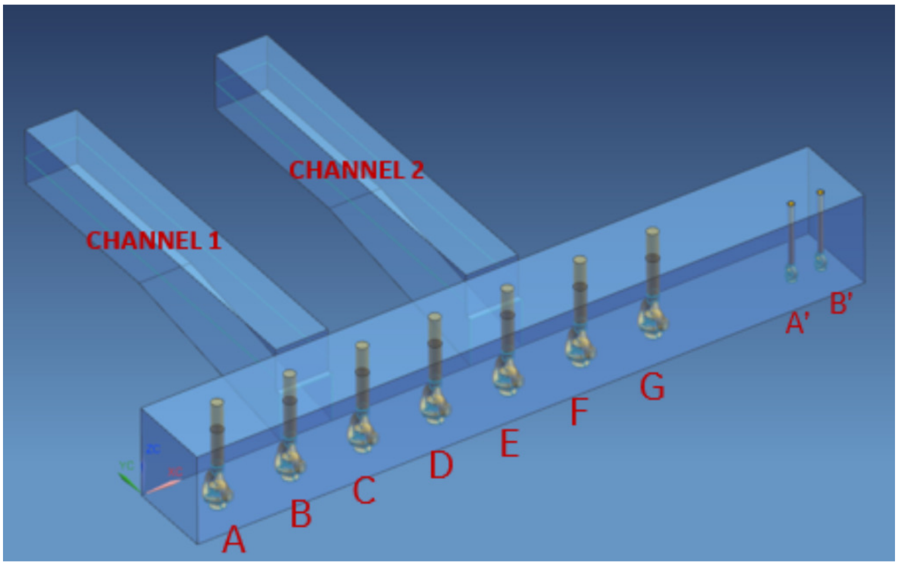

Fig.3 - Pumping Station Computational Domain.

In two of the test matrix configurations (7 and 9), which were classified as the most critical and representative from single phase calculation, an air-water interface has been modeled (Fig. 4).

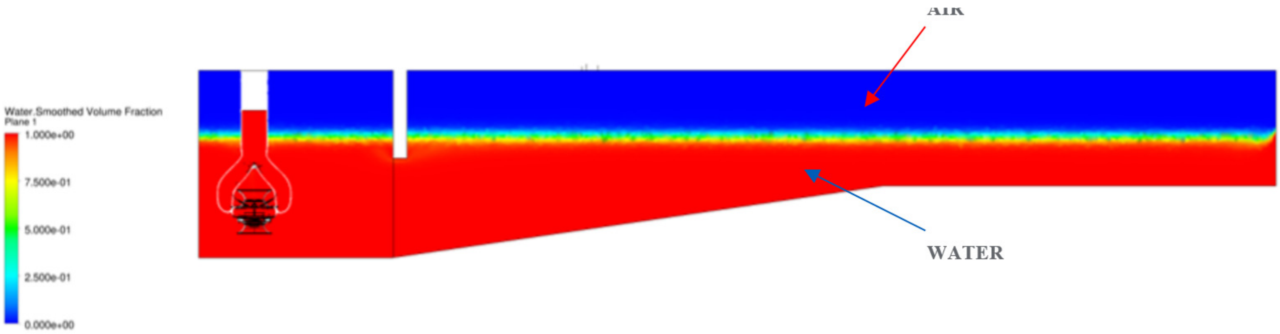

Fig.4 - Air-water interface.

To run calculation with two separated volumes of air (above free water level) and water, light modifications to model and some boundary conditions have been applied; specifically, mass flow rate and a reference pressure >50 kPa, (the value has been iteratively calculated using as first value the friction losses in the pump casing) at only one pump outlet and ambient pressure at free surface has been set. The reference pressure at pump outlet was tuned to reach the rated flow. Since the run time of air-water calculation was much higher than single phase and the main outcomes were mostly close we preferred to continue the CFD investigation using only single-phase approach.

CFD RESULTS

CFD results have been analyzed considering pre-swirl rotation, velocity profiles and vorticity development. High levels of vorticity are expected in areas with high velocity gradients. In order to visualize these areas, CFD vortex core regions have been drawn. A vortex feature identifies the domains where the vortex core should be found, nevertheless this is not a direct indication of air suction within the pumps. In the images below two working configurations (Figure 5(a) test configuration 7), Figure 5(b) test configuration 9) are reported showing potential vortex areas, specifically pump A in Figure 5(a) and both pump C and G in Figure 5(b).

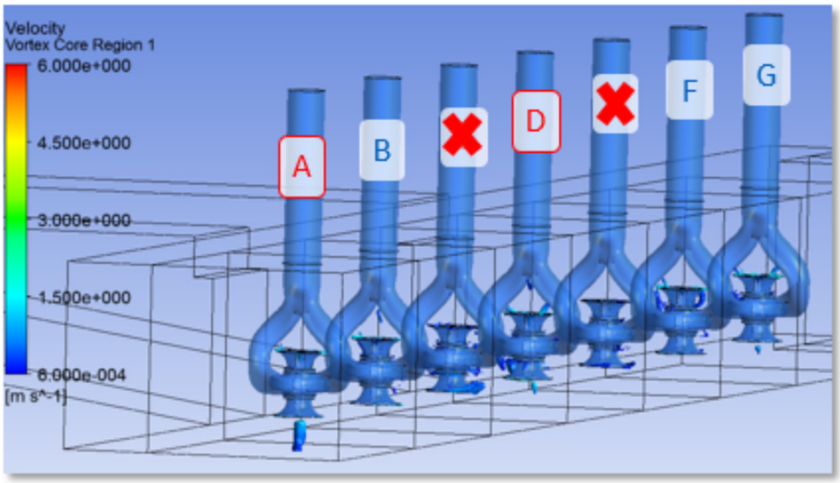

(a)

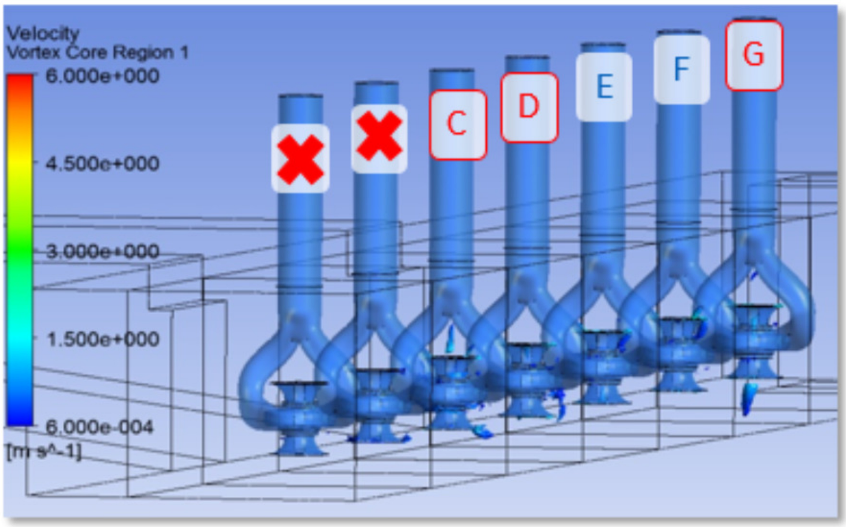

(b)

Fig.5 - Identification of submerged vortex.

Fluid streamlines, velocity vector plot and pre-swirl rotation are also studied to check potential critical areas as shown in Figure 6 (Test configuration 7) where swirling flows within the basin can be indicators of potential sub-surface vortex activity.

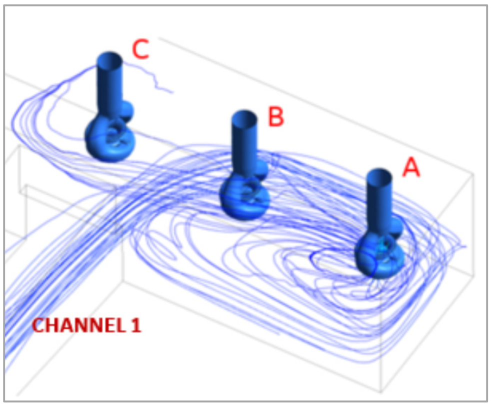

Fig.6 – Flow Streamlines test configuration 7.

The actual pre-swirl rotation is given by the swirl angle, that is a measure of the intensity of flow rotation at the impeller eye location due to upstream flow distribution. The swirl angle theta is calculated in CFD as arctan(V_R/V_A) at inlet throat area (Figure 7). Due to inlet flow distribution, local swirl angles are higher than ANSI/HI 9.8 recommended values (5°), while the mass flow averaged swirl angle on upper and lower bell at impeller eye area generally does not exceed the recommended value. The Figure 7 presents the flow patterns from CFD at each impeller eye for the main pump D in test configuration 7(as indicated in Fig 5a). Specifically, swirl angle, tangential and axial velocity distribution are shown for both the upper plane in Fig. 7 (a) and also the lower plane in Fig. 7 (b).

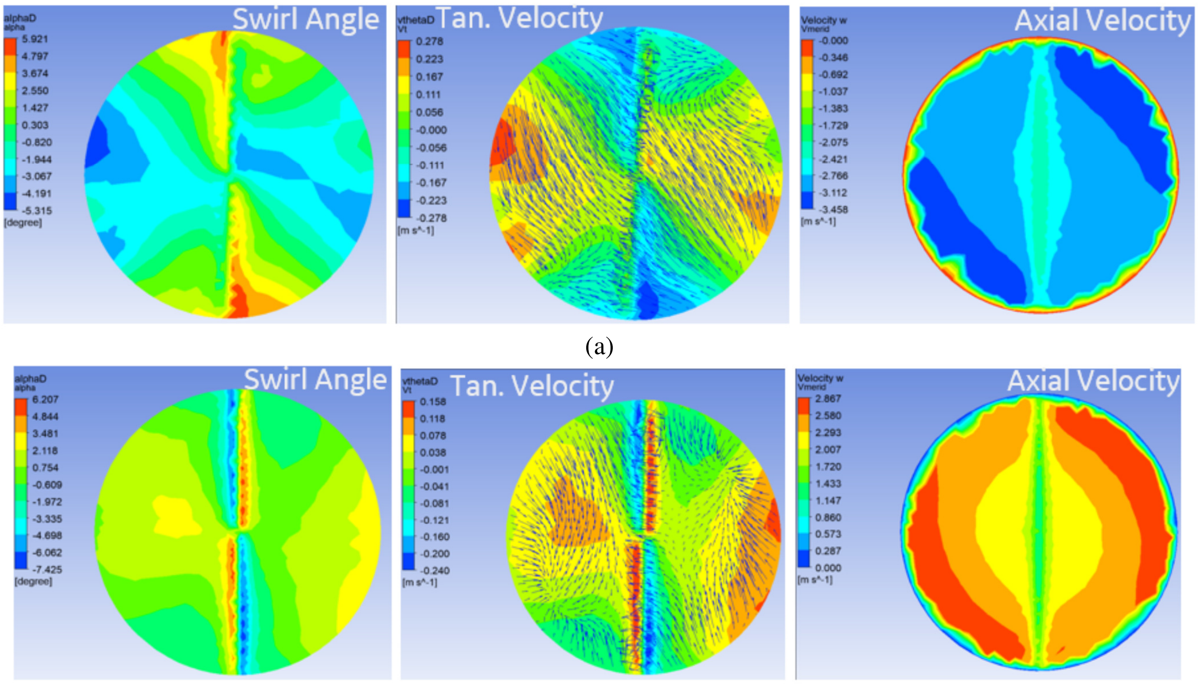

(a)

(b)

Fig. 7 – Pump A swirl and velocity distribution.

The local swirl in red and blue areas is respectively exceeding the values of +/- 7° while in the green areas the value of swirl angle does not exceed +/- 2°.
Some of those configurations, where the local pre-swirl at pump inlet given by CFD was above the recommended value [1], have been deeply investigated during model testing phase.
Table 4 shows mean and max values of axial velocity (Z component), at impeller inlet for the main pumps (test configuration 7), and their ratio that widely exceeds the recommended value of 10 percent.

Table 4 – Axial velocity at impeller inlet (test configuration 7).

Axial Velocity@Impeller Inlet						
Mean Axial Velocity [m/s]			**Max Velocity [m/s]**		**(Vmax-Vaverage)/Vaverage %**	
Pump	**Upper**	**Lower**	**Upper**	**Lower**	**Upper**	**Lower**
A	2.4	2.9	3.03	3.27	26.3%	12.8%
B	2.4	2.8	3.04	3.26	26.7%	16.4%
D	3	2.4	3.52	2.9	17.3%	20.8%
F	2.6	2.7	3.25	3.22	25.0%	19.3%
G	3.1	2	3.64	2.43	17.4%	21.5%

PHYSICAL MODELING OBJECTIVE

Objective of the model test was to construct and test a 1:5.4 scale model to validate CFD main outcomes and check potential risks associated with pit layout. A consultant specialized in creating large scale size physical models of cooling intake systems was contacted to investigate flow problems and propose solutions. Below the list of the activities carried-out during testing:

- Assessment of the hydraulic conditions generated in the pumping station in terms of inlet conditions and turbulence in the sumps under prescribed operating levels and pump operating combinations.
- Assessment of the approach flow patterns to the pump intakes.
- Swirl angle distribution at the impeller eye of each pump intake (top and bottom bell mouth) using a vortometer.
- Estimation of the degree of vortex activity (free and submerged) in the sump.
- Assessment of any air entrainment into the pump suction intakes due to areas of high surface turbulence or intense vortex activity.
- Assessment of uniformity of flow at the impeller eye using a pitot rake arrangement.
- Development of suggested modifications of pit layout such as fillet benching, dissipation columns, curtain walls, baffles, flow splitters and anti-vortex devices.

MODEL DESCRIPTION

A schematic P&ID of the physical model is shown in Figure 8.

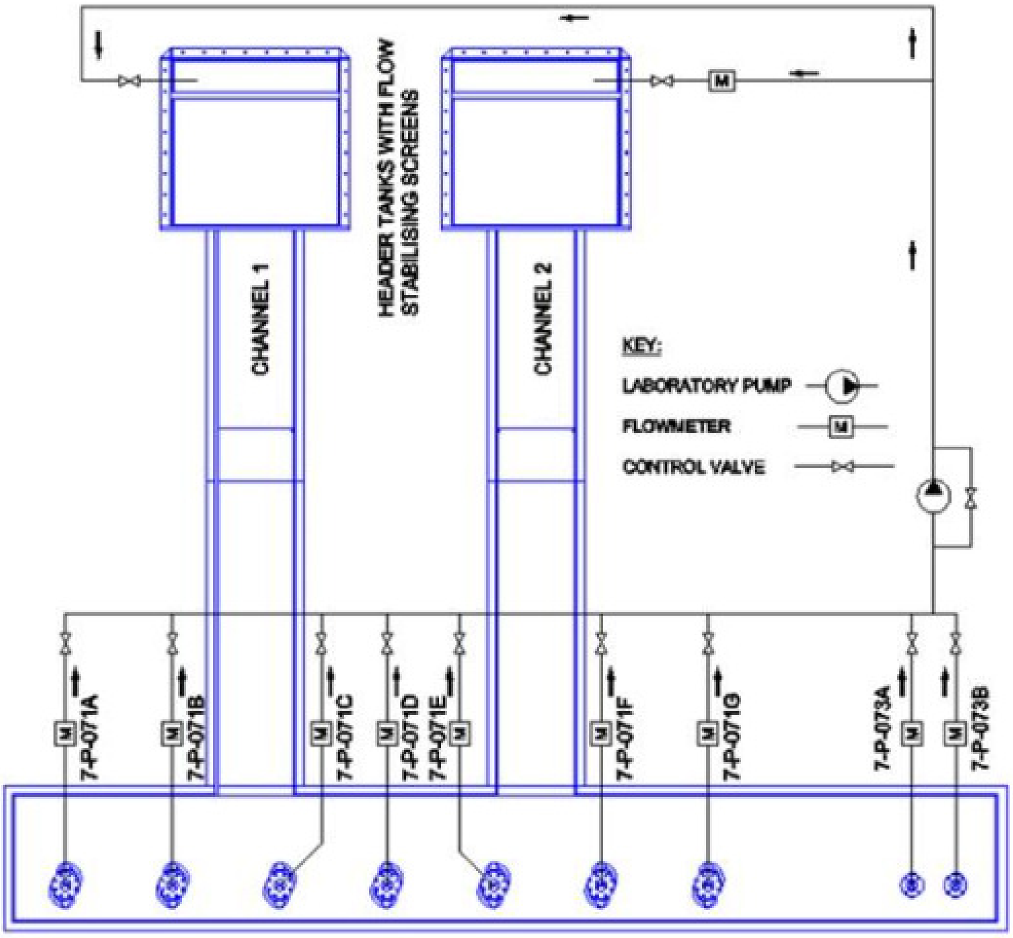

Fig. 8 – Model test P&ID.

Water was supplied to the model from header tanks located immediately upstream of the two inlet channel sections (Fig. 9 a)). Each of the courses trash gratings in the inlet channels were modelled as static structures (Fig. 9 b)) and Perspex® walls along one side of each inlet channel and the front of the sump were used to allow good viewing of flow patterns.

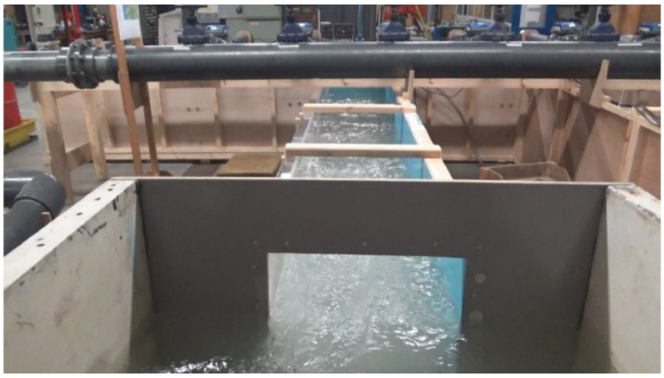

a) b)

Fig 9 - a) Header tank supply to channel 2 (without flow screen in place); b) Trash grating.

The geometry of each of the circulation and emergency pumps was modelled to represent essential external features (Figure 10). The external pump strainers that shrouded each pump were modelled to represent the flow conditioning of the prototype strainer with commercially available perforated sheets. Another feature of the model pump design was to have two vortometers free to rotate independently for each of suction bells to measure swirl at the eye of the pump impeller from both directions.

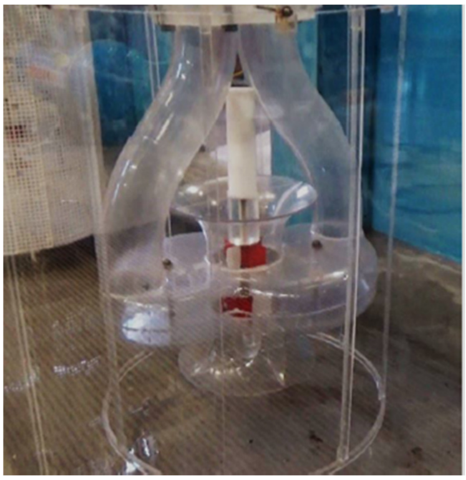

(a) (b)

Fig. 10. (a) Pump model w/o strainer; (b) Pump model with strainer.

INSTRUMENTATION AND MEASUREMENTS

Flow rate at discharge of each of the operating pumps was measured with mag flow meters. The flow at channel 2 was measured using M-channel and the flow at channel 1 by difference between the total flow and M-channel (Fig.8). The pump pre-swirl angle was measured by recording the rotation of vortometer vanes mounted at each pump's impeller eye (Figure 11). The swirl angle was determined using the following relationships:

$$\theta = \tan^{-1}\left(\frac{V_R}{V_A}\right) \quad (1)$$

The rotational velocity was determined from:

$$V_R = \frac{\pi d R}{60} \quad (2)$$

where d is the inner diameter of the section at the vortometer location and R the number of revolutions of the vane per minute. The axial velocity was determined from:

$$V_A = \frac{q}{A} \quad (3)$$

where q is the flow through each suction bell (assumed equal from top and bottom), and A is the cross-sectional area at the vortometer location. Swirl angle less than 5 degrees was considered as acceptable. Flow patterns at each impeller eye, sump walls and free surface level were observed with the aid of a dye tracer.

In test configuration 7, velocity traverse test was performed on pump D that was judged to have encountered the worst hydraulic conditions on final pit layout.

The design of the pitot rake was based on a representative "9 Pitot tube" layout, Figure 12. A differential pressure between the head of the Pitot tube normal to the flow and symmetrical taps (on the Pitot tube) parallel to the flow was used to calculate the velocity at the Pitot tube location. For this kind of measurement, the "9 Pitot tube" layout is less representative than the CFD calculation that is performed using entire impeller eye plane.

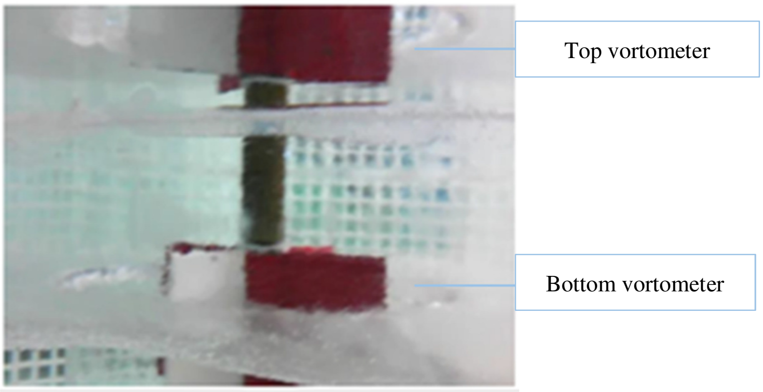

Fig. 11 - Two vortometers, top and bottom.

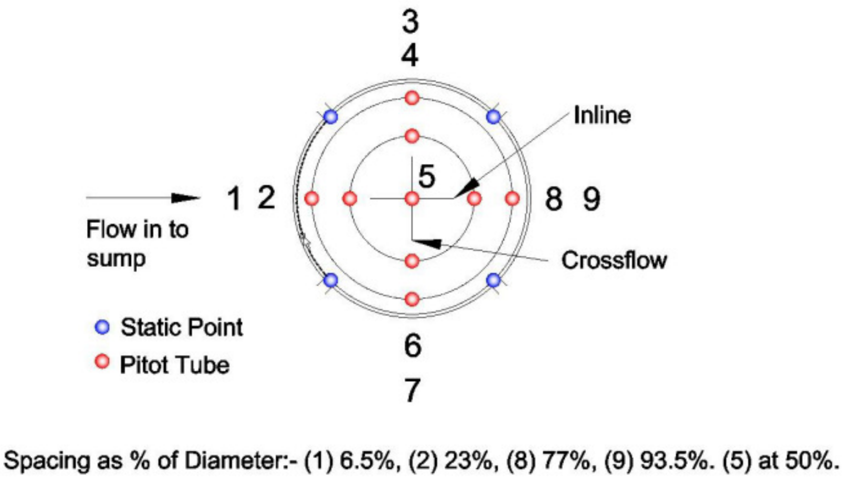

Fig. 12 - Standard 9 Pitot tube layout.

The formation of any potential air entraining or submerged vortices was observed and their classification noted in accordance with [1], Figure 13.

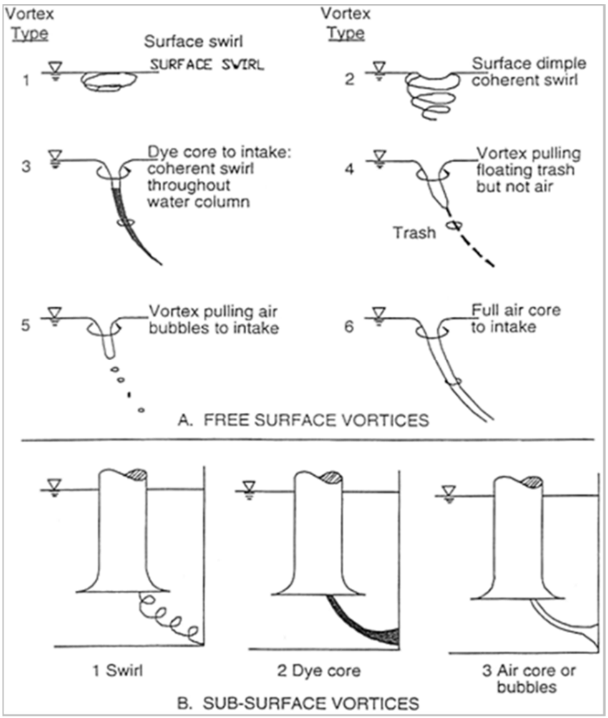

Fig. 13 - Vortex Type Classification [1].

MODEL TEST PROGRAM AND RESULTS

Performance of the pump station was investigated as designed and a few modifications were implemented to overcome any encountered problems. This was done by performing a test program divided into three sections, namely the initial tests, development of modifications and then final tests.

The hydraulic conditions in the inlet channels at low and high-water level did not lead to breaking of the water surface except when passing through the inlet trash screens. Any air entrainment from this did not reach the sump. At low water level operation surface vortex (type 5) activity drew entrained air from the ends of the inlet channels into the sump which could be carried to the pumps in the prototype (Figure 14).

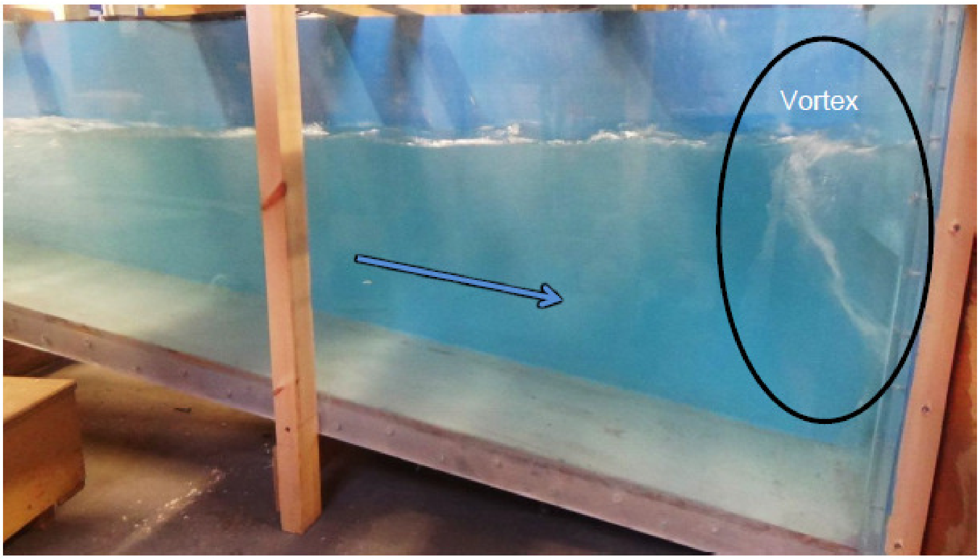

Fig. 14 – Vortex type 5 in the channel pulling air into the sump.

Hydraulic conditions in the sump were turbulent with strong rotating flow found under some strainers of operational pumps. Some flow patterns (in test configuration 7 and 10) are shown in Figure 15.

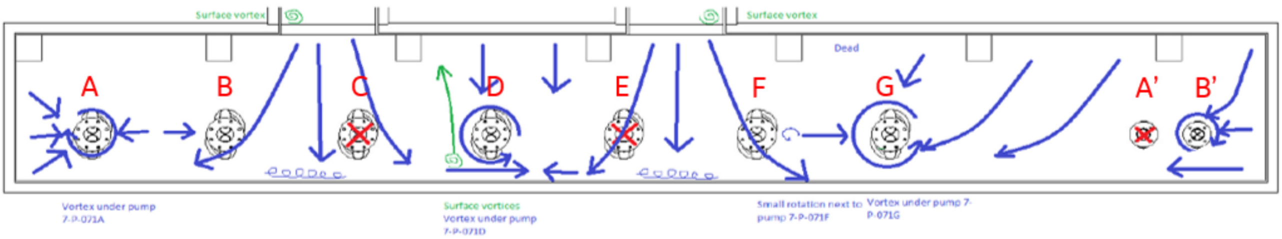

a)

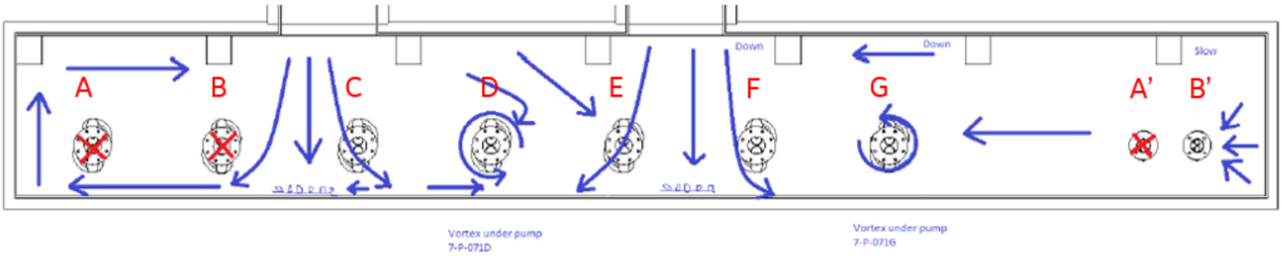

b)

Fig. 15: a) Flow pattern distribution in test configuration 7; b) Flow pattern distribution in test configuration 10.

One effect of the inlet jet from the left inlet channel, impacting on the front wall and visible in most of the configurations, was to create a spiraling flow between the front wall and the floor travelling to the side (Figure 16 a)). Different pump combinations did appear to influence local regions of flow patterns. This occasionally resulted in strong opposing flows creating eddies. Except for the surface eddies, no breaking of the water surface was found and no air entrainment generated in the sump. Nearly all the rotation observed that created a significant surface dimple (like that shown in figure 16 b)) was too-short-lived to develop into any definable or stable vortex structure.

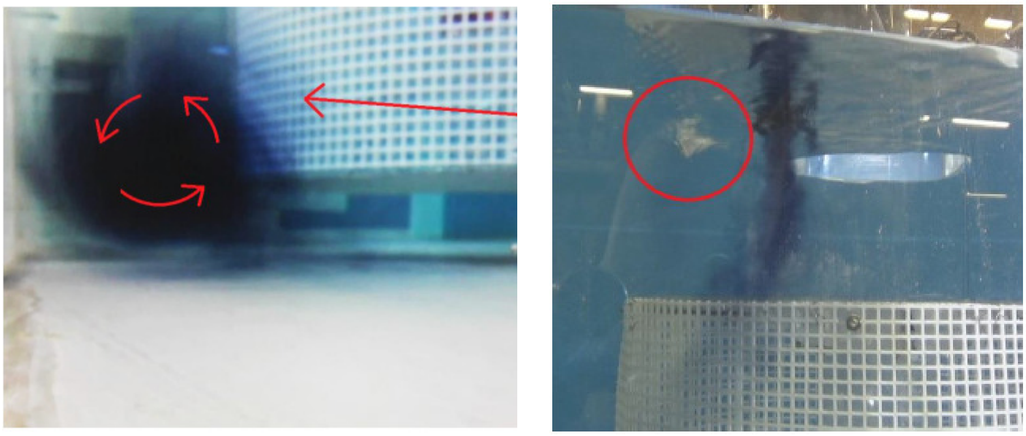

a) b)

Fig. 16. a) Inlet jet creating spiral flow visible in most of the configurations; b) Brief surface dimple highlighted in test configuration 7.

Under the bottom plate of the strainers of some pumps, strong intermittent but frequent rotations occurred, resulting in submerged type 2 vortex cores at times.

As already predicted by CFX simulation in configuration 7, as per Table 3, Pump D was exposed to multiple submerged vortex cores entering directly into the lower (Figure 17 a) and upper (Figure 17 b) bell-mouths from various locations. A summary table comparing CFD (vortex core) and physical model test vortex activity in the worst-case testing configurations is shown in Table 4.

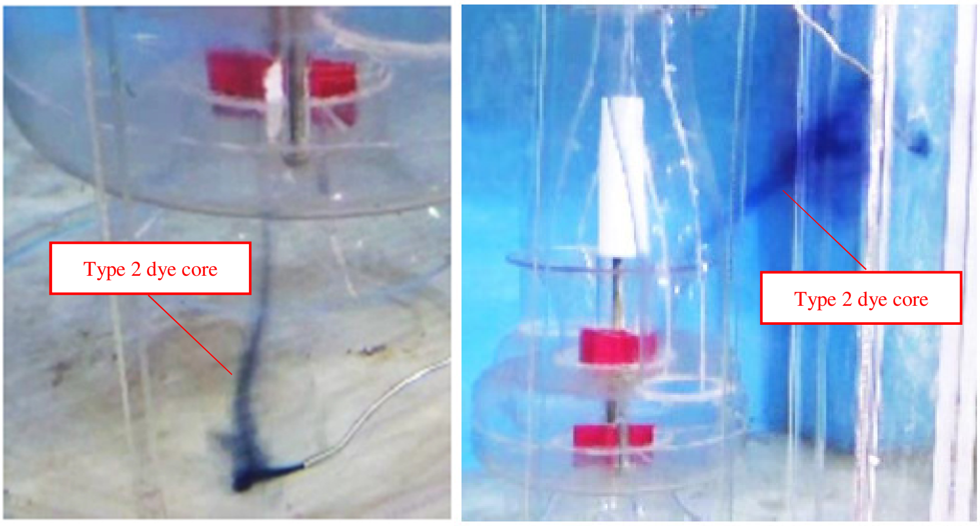

a) b)

Fig. 17. a) Submerged vortex entering lower bell-mouth of pump D, test configuration 7; b) Submerged vortex reaching upper bell-mouth of pump D, test configuration 7.

Operation without any modifications would have led to multiple vortex issues that would have directly impacted pump performance and reliability as discussed in previous chapters.

Some slight modification to pit lay out (columns at basin inlet and baffles between pumps) and to the pumps (modification to inlet pump strainers) were required acting as anti-vortex, cutting all vortex activity and stopping rotation of flow. After modifications, hydraulic conditions at pump inlet were improved presenting nearly uniform pattern of flow stream lines entering the suction bells (Figure 18). This resulted in swirl angles very much below the ANSI standard ($\theta<5°$) (see Table 5).

Table 4. Vortex activity with test configuration 7-8-9-10.

Test Conf	Circulating Pump													
	A		B		C		D		E		F		G	
	CFD	Model Test	CFD	Model Test	CFD	Model Test	CFD	Model Test	CFD	Model Test	CFD	Model Test	CFD	Model Test
7	++	++	-	-	not running		++	++	not running			-		++
8	++	++	-	-	-	-	+	++	+	-	not running		not running	
9	not running		not running		+	-	++	++	-	-	-	-	++	++
10	not running		not running		+	-	++	++	-	-	-	-	++	++

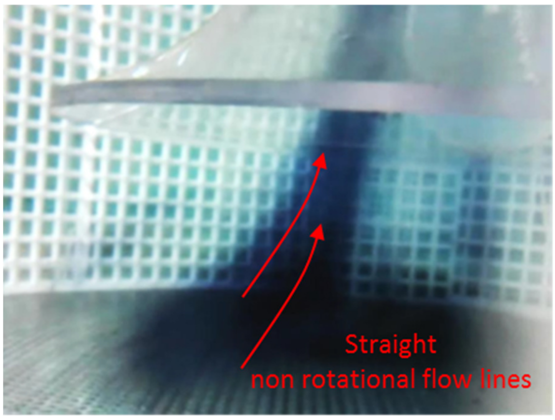

Figure 18. Non-rotational flow lines at pump inlet.

The air entraining vortex entering the sump from the inlet channel was ameliorated by placing a perforated plate with fine square mesh horizontally over the ends of the two straight channels next to sump (Figure 19). The screen cut off the vortex rotation and removed any vortex activity below the mesh.

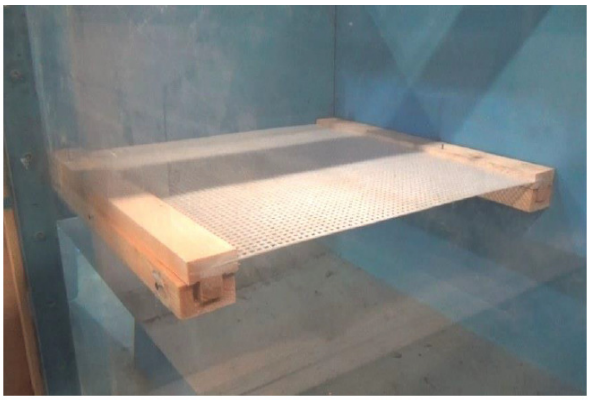

Figure 19. Anti-vortex screen over end of inlet channel.

Table 5 - Final tests pre-swirl with all modifications and screen.

Test Number	Bellmouth	Circulation Pumps, degrees													
		A		B		C		D		E		F		G	
1	Top	0.0	↔			0.1	↺			0.1	↻	0.2	↺	0.0	↔
	Bottom	0.6	↻			0.2	↻			0.0	↔	0.0	↔	0.1	↺
2	Top			0.0	↔			0.0	↔	0.1	↻	0.2	↻	0.0	↔
	Bottom			0.3	↻			0.0	↔	0.2	↻	0.0	↔	0.0	↔
3	Top	0.1	↺	0.0	↔	0.1	↔	0.1	↺			0.1	↺		
	Bottom	0.5	↻	0.1	↻	0.0	↔	0.1	↻			0.0	↔		
4	Top	0.1	↺	0.0	↻	0.1	↺			0.1	↺			0.0	↔
	Bottom	0.4	↻	0.2	↻	0.0	↔			0.0	↔			0.1	↺
5	Top			0.0	↔	0.1	↺	0.1	↺	0.1	↺	0.1	↺		
	Bottom			0.3	↻	0.2	↻	0.0	↔	0.0	↔	0.0	↔		
6	Top	0.1	↺			0.0	↔	0.1	↺	0.1	↺			0.0	↔
	Bottom	0.6	↻			0.1	↻	0.0	↔	0.0	↔			0.1	↺
7	Top	0.1	↺	0.0	↔			0.1	↺			0.1	↺	0.0	↔
	Bottom	0.1	↻	0.2	↻			0.1	↺			0.0	↔	0.1	↺
8	Top	0.1	↻	0.0	↔	0.1	↺	0.1	↺	0.1	↻				
	Bottom	0.4	↻	0.2	↻	0.0	↺	0.0	↔	0.0	↔				
9	Top					0.1	↻	0.0	↔	0.1	↺	0.1	↺	0.0	↔
	Bottom					0.1	↺	0.0	↔	0.0	↔	0.0	↔	0.1	↺
10	Top					0.1	↻	0.0	↔	0.1	↺	0.1	↺	0.0	↔
	Bottom					0.1	↺	0.0	↔	0.0	↔	0.0	↔	0.1	↺

The results for the two perimeter arrays of Pitot tubes in configuration 7 pump D, were within the 10 percent margin of acceptability and were consistent for both the upper and lower bellmouth and the velocity profiles were mostly uniform.

CONCLUSIONS AND RECOMMENDATIONS

The investigated geometry of pit layout was critical for safe pumps operation due to some dimensions out of recommended limits by ANSI/HI 9.8-2012. Combined CFD study and Physical Model Testing activity confirmed the potential problems associated to basin dimensions and permitted to find out and evaluate possible solutions.
The CFD study allowed to identify some key conclusions:

- Vortex regions visualization show the potential presence of vortices on Main Pumps in most of simulated configurations.
- Vortex indicator shows a higher value in testing configurations in which four working main pumps or more are close to each other.
- Local swirl angles were higher than recommended values.
- On the emergency pumps no relevant indications are shown since far from the adduction channels the flow is better

distributed along the pit.

- Local modifications to the sump pit, such as columns and baffles at the adduction channel outlet, can help to improve the pumps' intake flow distribution and smooth recirculation areas. Some of these modifications were successfully implemented during "development of modifications phase" in model testing activities, making both the swirl angles and the axial velocity patterns at each impeller eye fully complying with Standards [1]

CFD information have been used to support physical modelling testing phase. Most of the modifications coming from CFD were directly applied and confirmed by Physical Model Test.
This combined approach helped to achieve effective solutions, reducing the number of iterations during Physical Model Testing phase and minimizing time and costs.

NOMENCLATURE

A	= Inlet area	[m^2]
C	= Distance between suction bell and pit bottom	[m]
D	= Bell diameter	[m]
d	= Diameter of pump intake in scaled model	[m]
Fr	= Froude Number	
g	= Gravitational acceleration	[m/s^2]
P	= Pressure	[bar]
Q	= Flow rate	[m^3/h]
q	= Flow inlet	[m^3/h]
R	= Number of revolutions per minute of vortometer	
Re	= Reynolds Number	
S	= Minimum submergence	[m]
u	= Velocity at suction inlet	[m/s]
V_A	= Mean axial velocity at impeller inlet	[m/s]
V_R	= Mean rotational velocity at impeller inlet	[m/s]
We	= Weber Number	
θ	= Circulation of the flow	
ν	= Kinematic viscosity of the liquid	[cSt]
ρ	= Liquid density	[kg/m^3]
σ	= Surface tension of liquid/air interface	[N/m]

REFERENCES

[1] American National Standard for Pump Intake Design, *Hydraulic Institute, ANSI/HI 9.8 – 2012*.

[2] Schiavello B., Smith D.R., Price S.M. 2004, "Abnormal vertical pump suction recirculation problems due to pump-system interaction", *Proc. 21st International Pump Users Symposium*, Houston, TX, pp. 18-47.

[3] Daggett, L. L. and Keulegan, G. H. 1974, "Similitude in free-surface vortex formations", *ASCE Journal of the Hydraulics Division*, HY11.

[4] Jain, A. K., Raju, K. G. R., Garde, R. J. 1978, "Vortex formation at vertical pipe intakes", *ASCE Journal of the Hydraulics Division*, HY10.